Nonlinear delayed symmetry breaking in a solid excited by hard x-ray free electron laser pulses

A. Ferrer,[1,2,a)] J. A. Johnson,[2,b)] T. Huber,[1] S. O. Mariager,[2] M. Trant,[1] S. Grübel,[2] D. Zhu,[3] M. Chollet,[3] J. Robinson,[3] H. T. Lemke,[3] G. Ingold,[2,4] C. Milne,[4] U. Staub,[2] P. Beaud,[2,4] and S. L. Johnson[1,c)]
[1]*Institute for Quantum Electronics, ETH Zurich, CH-8093 Zurich, Switzerland*
[2]*Swiss Light Source, Paul Scherrer Institut, CH-5232 Villigen PSI, Switzerland*
[3]*LCLS, SLAC National Accelerator Laboratory, Menlo Park, California 94025, USA*
[4]*SwissFEL, Paul Scherrer Institut, CH-5232 Villigen PSI, Switzerland*

(Received 21 January 2015; accepted 2 April 2015; published online 13 April 2015)

We have studied the ultrafast changes of electronic states in bulk ZnO upon intense hard x-ray excitation from a free electron laser. By monitoring the transient anisotropy induced in an optical probe beam, we observe a delayed breaking of the initial c-plane symmetry of the crystal that lasts for several picoseconds. Interaction with the intense x-ray pulses modifies the electronic state filling in a manner inconsistent with a simple increase in electronic temperature. These results may indicate a way to use intense ultrashort x-ray pulses to investigate high-energy carrier dynamics and to control certain properties of solid-state materials. © *2015 AIP Publishing LLC*.
[http://dx.doi.org/10.1063/1.4917506]

Light-induced control over the properties of solid-state materials has attracted considerable attention.[1–7] In the ultraviolet (UV), optical, and near-infrared regions of the electromagnetic spectrum, the dominant interaction is usually with electronic states on the order of 1 eV above the Fermi level.[8–10] These electronic states can couple to atomic or magnetic structure, allowing some level of coherent control via an indirect Raman mechanism.[11,12] In the mid- and far-infrared range of the spectrum, it becomes possible to directly couple to infrared-active excitations. Such mechanisms for control have recently been demonstrated in multiferroics[6] and in strongly correlated systems in the vicinity of phase transitions.[13,14] Excitation using higher frequencies extending from the deep-UV to hard x-rays, however, remains largely unexplored for solid-state systems, mainly due to the limited availability of intense ultrafast sources.

The advent of x-ray free electron lasers (XFELs)[15–18] now allows us to address the question of how high energy photons can be used to alter the state of condensed phase systems. Pumping with x-rays allows access to new states and nearly arbitrary regions of the Brillouin zone. For example, x-ray photon energies near core-level binding energies provide a way to create highly localized, element-specific excitations. This is simply not possible with optical frequency photons, where the low energy and momentum of photons restrict the excitations to nearly the center of the Brillouin zone.

In principle, the interaction of solids with intense x-rays might be expected to parallel interactions observed at lower frequencies, but this remains to a large extent experimentally unexplored.[19,20] X-ray pump experiments have so far mainly focused on ablation studies[21,22] and as a diagnostic tool to correct for random jitter between the FEL and laser pulses.[23–28] In the latter experiments, an ultrafast change in transmission or reflectivity of a sample upon hard x-ray excitation is measured in a single shot configuration. Phenomenologically, this change is often modelled as a step function that slowly recovers to the initial value before time zero. For the majority of currently implemented schemes for measuring timing jitter, this phenomenological treatment is sufficient, since the precise shape of the optical response as a function of time is not directly relevant. The actual dynamics of the electronic response, however, becomes important in schemes where the effect is used to measure the pulse duration of XFEL pulses.[24] This application of x-ray/optical cross correlators relies on the validity of a physical model where the x-ray excited carriers in a transparent insulator induce a highly excited and thermalized electron-hole plasma state that slowly relaxes to the ground state. In this work, we present results that challenge this assumption for some systems, specifically in the case of ZnO.

Another key question concerning the interaction of intense x-rays with solids is whether it is possible to use x-ray pulses to drive a persistent change in the symmetry of a material. This could potentially lead to novel schemes of phase or domain control in solids. In the optical regime optical excitation schemes, such as impulsive stimulated Raman scattering (ISRS), have been shown to drive symmetry-breaking coherent phonon modes in crystals,[12] relaxation dynamics in liquids,[29] and rotational and vibrational motions in gases.[30,31] Optical excitation has also been shown to induce ultrafast anisotropy in the momentum distribution of excited electronic carriers in graphene.[32]

To investigate the possibility of similar symmetry-breaking processes with x-rays, we have conducted measurements of the transient optical properties of a single crystal of ZnO excited by an intense x-ray pump pulse from a free

a)Electronic mail: aferrer@phys.ethz.ch
b)Electronic mail: jjohnson@chem.byu.edu
c)Electronic mail: johnson@phys.ethz.ch

electron laser. The experiment has been performed at the XPP instrument at the LCLS FEL.[15]

ZnO is a wurtzite II-VI semiconductor with a large bandgap (≈3.37 eV), which makes ZnO a good candidate for high frequency light emitting devices. It has a very large exciton binding energy (≈60 meV), which makes excitonic emission possible even at room temperature. These properties together with a large polarizability and the mixed polar and ionic character of the Zn-O bond result in strong light matter interaction effects.

ZnO is a birefringent uniaxial crystal.[33] Structurally, it is a relatively simple system that can be grown as a single bulk crystal in the hexagonal wurtzite structure. It consists of Zn and O planes, alternately stacked along the c-axis. ZnO belongs to the space group C_{6v}^4 and consists of 4 atoms per unit cell, leading to 12 vibrational eigenmodes. The lowest energy phonon mode (2.97 THz) corresponds to a pair of degenerate E modes, usually referred to as E_2^{low} in the literature.[34] When coherently excited with sufficiently short pulses of linearly polarized light (via ISRS), this phonon mode breaks the symmetry in the c-plane and modulates temporally the dielectric tensor of the material. These modulations can be experimentally measured using standard transient birefringence or transmission probes.[35]

With ZnO as a model system, we have performed a pump-probe experiment with the aim to understand the changes induced by strong excitation with femtosecond pulses of light in the hard x-ray regime. Pump induced transient anisotropy in the sample is monitored using a polarization gating detection scheme, similar to that used in optical Kerr effect and electro-optic sampling measurements.[36,37] We observe complex relaxation dynamics showing a strongly non-linear, hard x-ray induced anisotropy.

The sample is a commercial c-cut ZnO single crystal, with dimensions 5 mm × 5 mm × 0.2 mm. Both (001) facets are polished to optical grade. As depicted in Figure 1, the hard x-ray (6.67 keV) pump beam is focused down to 15 μm $1/e^2$ diameter at the sample position and meets the Bragg condition for diffraction from the (210) ZnO planes. The detection setup is similar to a standard optical Kerr effect setup. A linearly polarized 800 nm laser beam (45 fs FWHM pulse duration) is focused at normal incidence onto the surface of the sample ($1/e^2$ spot diameter of 140 μm and pulse energy of 0.7 μJ). The large probe size as compared to the pump beam size ensures spatial overlap despite the pointing

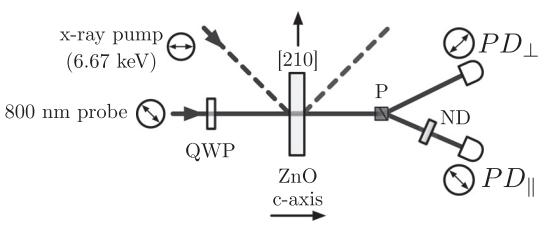

FIG. 1. Schematic of the hard x-ray pump (6.67 keV)-800 nm probe experimental setup. The orientation of the (linear) polarization of each beam is outlined at different stages of the set up with arrows enclosed in circles. P is a Glan Laser polarizer with a 10^{-5} extinction ratio. QWP is a quarter wave plate. The x-ray pump is incident at 61° with respect to the surface normal and the 800 nm probe at normal incidence.

instability present in the x-ray pump beam. The probe beam is polarized at 45° with respect to the pump beam polarization. A quarter wave plate (QWP) placed before the sample is initially aligned with its fast axis along the probe beam polarization. Under these geometrical conditions, the group velocities of pump and probe beams are matched. We observe similar dynamics when slightly detuning the sample out of this x-ray diffraction condition. The shot-to-shot fluctuation of the incident pump intensity is larger than 100%. It is monitored upstream allowing all the data to be grouped into bins of varying pump excitation levels.

After the sample, the probe beam passes through a Glan Laser polarizer (P), which is crossed with respect to the initial laser beam polarization. The two beams coming out of P are delivered to two photodiodes to record the crossed ($PD_\perp$) and parallel ($PD_\parallel$) polarizations (relative to initial polarization of the probe beam). The QWP is rotated slightly to minimize the increase of light going to $PD_\perp$ after inserting the sample at normal incidence in the probe beam. In this configuration, the QWP partially compensates for the residual birefringence of the ZnO sample, which we attribute to strain.[38] The angle of the QWP is then $\alpha = 0°$. An additional rotation of the QWP may introduce a local oscillator allowing heterodyne detection of the signal.[36,37] A set of such heterodyne results are shown in the supplementary material.[38] A bandpass filter together with absorptive neutral density filters are placed in front of the photodiodes (not shown). These serve both to block the photoluminescence of the sample and to attenuate the probe beam in order to prevent saturation of the photodiodes. An additional reflective variable filter is placed just before the $PD_\parallel$ photodiode in order to attenuate the light and make it equal in magnitude to that of the $PD_\perp$ channel for balanced detection.

A mechanical delay line introduces an average controllable delay between pump and probe pulses. A single-shot x-ray/laser cross correlation installed at the XPP endstation[25] measures the fluctuations in the relative timing between the pump and the probe pulses. The data are afterwards corrected for temporal jitter.

The normalized change in transmission for each of the two polarizations is shown in Figs. 2(a) and 2(b). The colors of the time traces correspond to different pump fluences. The ratio of the two photodiode signals is shown in Figure 2(c). To leading order, the signals in Figures 2(a) and 2(b) are proportional to the overall transmission of the sample as well as the probe laser shot-to-shot fluctuations. The photodiode $PD_\perp$ is in addition proportional to the anisotropy introduced by the sample,[38] a situation that happens only upon symmetry breaking in the c-plane. The ratio (Fig. 2(c)) is a pure anisotropic signal, since the isotropic change in transmission has been removed after dividing the two constituent signals.[38]

As shown in Fig. 2, ZnO presents rich anisotropic and isotropic responses upon hard x-ray pump as a function of probe delay, which we divide into three ranges: (i) *time zero anisotropy*, (ii) *delayed anisotropy* (comprising pump-probe delays between ≈1.6 ps and ≈8 ps), and (iii) *isotropic response* (time delays $t > 8$ ps according to the ratio shown in 2(c)).

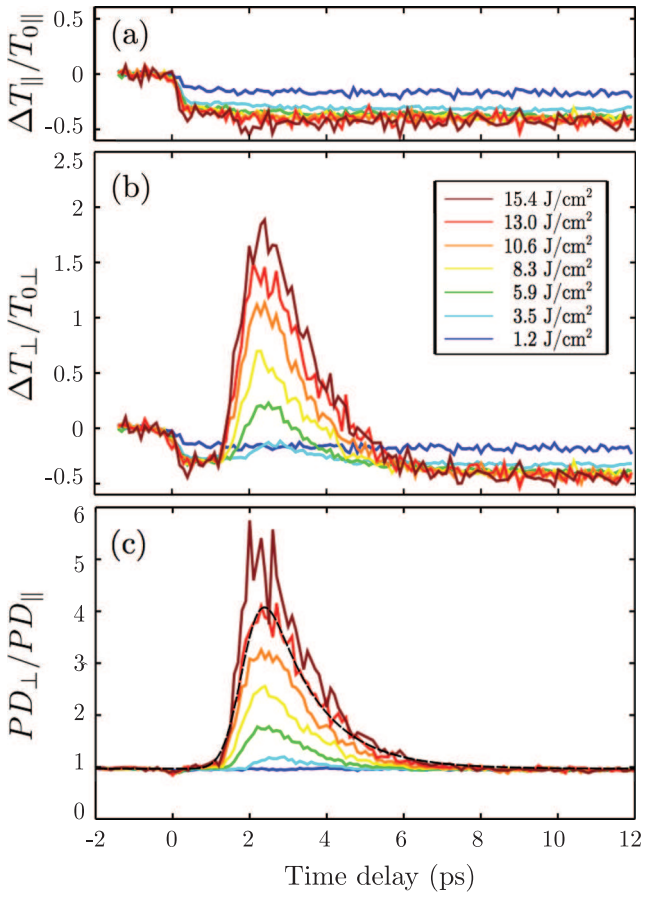

FIG. 2. Normalized change in transmission for parallel (a) and perpendicular (b) polarization channels for different fluences (colors) as a function of the temporal delay between the hard x-ray pump (6.67 keV) and optical probe at 800 nm. (c) Transient anisotropy data and representative fit to the expression $y_0 + \frac{A}{2}\{1 + \mathrm{erf}[\sqrt{2}(t-t_0)/\sigma]\} \times \exp(-(t-t_0)/\tau)$, for fluence of 13.0 J/cm^2 (black dashed line).

(i) *Time zero anisotropy:* A small negative spike is observed in the vicinity of time zero even for the traces at low pump fluences (Fig. 2(c)). After this short time-zero spike, there seems to be an *induction time* of about 1.6 ps, where no anisotropy is generated in the probe beam.

(ii) *Delayed anisotropy:* The most striking response of the material appears at time delays ranging from 1.6 ps to 8 ps. An increase in the signal is observed after an approximately 1.6 ps induction time. This delayed anisotropic response also appears only above a critical fluence.

In order to quantify this behavior, the traces in Fig. 2(c) have been fitted to the phenomenological function $y_0 + \frac{A}{2}\{1 + \mathrm{erf}[\sqrt{2}(t-t_0)/\sigma]\} \times \exp(-(t-t_0)/\tau)$, where erf is the Gauss error function, y_0 is a vertical offset, A is proportional to the amplitude of the anisotropy signal, t is the time delay, t_0 is the time offset for the anisotropy signal, and σ and τ are the time constants for the rise and the fall, respectively. One representative fit is shown in Figure 2(c) (dashed line), while the complete set of fits is shown in the supplementary material.[38] The retrieved amplitude A is plotted in Figure 3 as a function of the pump fluence. The amplitude remains close to zero below a critical pump fluence (3.48 ± 0.97 J/cm^2) and increases linearly after this threshold.

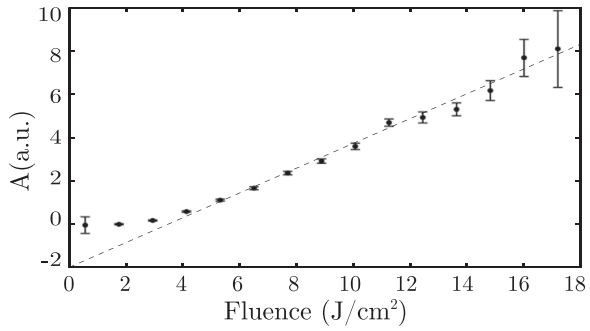

FIG. 3. Amplitude of the anisotropy signal A as a function of the of the pump fluence. The error bars correspond to 95% confidence bounds of the fitting parameter. The dashed line is a linear fit to the points above 2 mJ/cm^2.

(iii) *Isotropic response:* At later times, i.e., after 8 ps, the anisotropy signal has fully decayed and only an isotropic change in transmission remains. In order to quantify this change, we have averaged the last 4 ps of each trace in Figure 2(a) (it is equivalent for the traces shown in Fig. 2(b)) and fitted it to an exponential decay as a function of the pump fluence. The results are shown in Fig. 4. The isotropic normalized change in transmission saturates at level close to 41%. This would correspond to a complete block of the probe transmission over a centered circular region of 36 μm in diameter.

We begin the discussion with a short description of the x-ray excitation of carriers. Hard x-ray absorption takes place in atomic shallow core states and valence electrons, leading to the ejection of highly excited electrons. Each ejected electron may traverse many crystal unit cells, leaving potentially thousands more highly excited electrons in its wake due to impact ionization. The highly excited electrons can lose energy through Auger processes, impact ionization, electron-electron scattering processes, and eventually recombination. Theoretical studies on silicon showed that in the hard x-ray regime, most excited carriers are created through impact ionization processes,[39] with the excited carrier concentration reaching a maximum within tens of femtoseconds for an intense 13 fs FWHM 8 keV x-ray pump pulse.

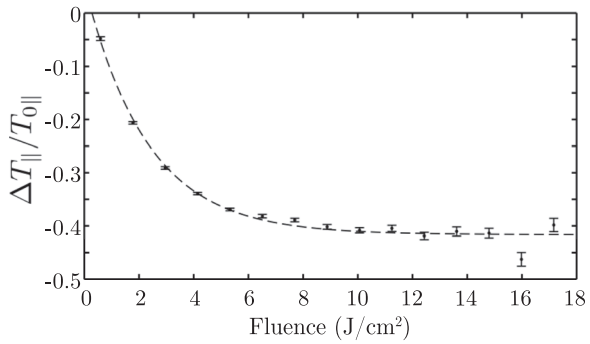

FIG. 4. Normalized change in the transmission of the parallel polarization as a function of the of the pump energy, averaged from 8 to 12 ps. The error bars correspond to the standard error. The dashed line is a single exponential decay fit.

The time zero anisotropy consists of a negative spike. We attribute this (potentially experimental time-resolution-limited) effect to the anisotropy of the initial excitation with linear polarization of the hard x-ray pump. In other hexagonal materials like graphene, it has been shown, both theoretically[40–42] and experimentally,[32] that linear polarization of pump radiation can break the symmetry of the system by creating an excited carrier population with an anisotropic momentum distribution, with maxima in the momentum perpendicular to the pump polarization direction. The isotropic signal immediately after the time zero response could potentially be because the carrier momentum distribution has become randomized and isotropic or potentially also because the high energy carriers simply do not contribute to the ZnO optical properties at the 800 nm probe light frequency.

As described above, after a 1.6 ps delay, a strong delayed anisotropic signal appears in the crossed polarized channel. Such an effect has not been previously reported in the literature and its origins are unclear. In nanostructured ZnO, a delayed appearance of photoluminescence (at similar timescales) appears after pumping with 266 nm light.[43] In that case, it is attributed to the radiative relaxation of the electron-hole plasma formed in that material. However, there is so far no evidence of how such a process of formation and relaxation of an electron hole plasma would be related to a symmetry breaking in the c-plane. In graphene, upon interband excitation, an anisotropic carrier population generation and detection as well as evidence for collinear anisotropy-preserving electron-electron scattering has been demonstrated.[32] But in this case, the anisotropic response appeared instantaneously and subsequent thermalization leading to a loss of anisotropy occurred within tens of femtoseconds. Simulations of the x-ray excitation and subsequent relaxing of high energy carriers, such as those performed on silicon,[39] may be required to fully understand the intriguing, delayed electronic symmetry breaking observed here in ZnO.

In conclusion, we have found that the relaxation dynamics of the electronic system in bulk ZnO is strongly anisotropic when excited with linearly polarized hard x-rays, and that it cannot be described by a simple electronic temperature rise. This result suggests that, at least in the case of ZnO, the previously held assumptions that the x-ray excited electrons in an insulator form a thermalized, isotropic plasma on a time scale of a few 10 s of femtosecond may not be completely correct.[24] Furthermore, this anisotropic behavior could not be observed with standard transmission or reflection probe setups (e.g., timing tool measurements[23–28]), since it requires a careful choice and analysis of the polarizations of the pump and probe beams. Further experiments are needed to more fully understand the induction time and the anisotropic dynamics in ZnO, as well as the possibility of similar symmetry breaking dynamics in materials commonly used in jitter correction measurements. Such studies may well provide insights into new phenomena in solid state materials made possible with XFEL facilities as well as an improvement in existing diagnostic tools.

This research was carried out on the XPP Instrument at the LCLS, a division of SLAC and an Office of Science user facility operated by Stanford University for the U.S. Department of Energy (DOE). This work was supported by the NCCR Molecular Ultrafast Science and Technology (NCCR MUST), a research instrument of the Swiss National Science Foundation (SNSF). A.F. acknowledges financial support from the Marie-Curie PSI-Fellow CoFund program. J. A. Johnson was supported in part by the Marie Curie Actions IFP-MUST Cofund.

[1]K. Sokolowski-Tinten, C. Blome, J. Blums, A. Cavalleri, C. Dietrich, A. Tarasevitch, I. Uschmann, E. Förster, M. Kammler, M. Horn-von Hoegen, and D. von der Linde, Nature **422**, 287 (2003).
[2]A. Kirilyuk, A. V. Kimel, and T. Rasing, Rev. Mod. Phys. **82**, 2731 (2010).
[3]M. Först, C. Manzoni, S. Kaiser, Y. Tomioka, Y. Tokura, R. Merlin, and A. Cavalleri, Nat. Phys. **7**, 854 (2011).
[4]D. Daranciang, M. J. Highland, H. Wen, S. M. Young, N. C. Brandt, H. Y. Hwang, M. Vattilana, M. Nicoul, F. Quirin, J. Goodfellow, T. Qi, I. Grinberg, D. M. Fritz, M. Cammarata, D. Zhu, H. T. Lemke, D. A. Walko, E. M. Dufresne, Y. Li, J. Larsson, D. A. Reis, K. Sokolowski-Tinten, K. A. Nelson, A. M. Rappe, P. H. Fuoss, G. B. Stephenson, and A. M. Lindenberg, Phys. Rev. Lett. **108**, 087601 (2012).
[5]S. L. Johnson, R. de Souza, U. Staub, P. Beaud, E. Möhr-Vorobeva, G. Ingold, A. Caviezel, V. Scagnoli, W. Schlotter, J. Turner, O. Krupin, W. S. Lee, Y. D. Chuang, L. Patthey, R. Moore, D. Lu, M. Yi, P. Kirchmann, M. Trigo, P. Denes, D. Doering, Z. Hussain, Z. X. Shen, D. Prabhakaran, and A. Boothroyd, Phys. Rev. Lett. **108**, 037203 (2012).
[6]T. Kubacka, J. A. Johnson, M. C. Hoffmann, C. Vicario, S. de Jong, P. Beaud, S. Grübel, S. W. Huang, L. Huber, L. Patthey, Y. D. Chuang, J. J. Turner, G. L. Dakovski, W. S. Lee, M. P. Minitti, W. Schlotter, R. G. Moore, C. P. Hauri, S. M. Koohpayeh, V. Scagnoli, G. Ingold, S. L. Johnson, and U. Staub, Science **343**, 1333 (2014).
[7]P. Beaud, A. Caviezel, S. O. Mariager, L. Rettig, G. Ingold, C. Dornes, S. W. Huang, J. A. Johnson, M. Radovic, T. Huber, T. Kubacka, A. Ferrer, H. T. Lemke, M. Chollet, D. Zhu, J. M. Glownia, M. Sikorski, A. Robert, H. Wadati, M. Nakamura, M. Kawasaki, Y. Tokura, S. L. Johnson, and U. Staub, Nat. Mater. **13**, 923 (2014).
[8]M. A. M. Versteegh, T. Kuis, H. T. C. Stoof, and J. I. Dijkhuis, Phys. Rev. B **84**, 035207 (2011).
[9]V. M. Axt and T. Kuhn, Rep. Prog. Phys. **67**, 433 (2004).
[10]F. Rossi, Rev. Mod. Phys. **74**, 895 (2002).
[11]T. Stevens, J. Kuhl, and R. Merlin, Phys. Rev. B **65**, 144304 (2002).
[12]R. Merlin, Solid State Commun. **102**, 207 (1997).
[13]A. Subedi, A. Cavalleri, and A. Georges, Phys. Rev. B **89**, 220301 (2014).
[14]A. Cavalleri, C. Tóth, C. Siders, J. Squier, F. Ráksi, P. Forget, and J. Kieffer, Phys. Rev. Lett. **87**, 237401 (2001).
[15]C. Bostedt, J. D. Bozek, P. H. Bucksbaum, R. N. Coffee, J. B. Hastings, Z. Huang, R. W. Lee, S. Schorb, J. N. Corlett, P. Denes, P. Emma, R. W. Falcone, R. W. Schoenlein, G. Doumy, E. P. Kanter, B. Kraessig, S. Southworth, L. Young, L. Fang, M. Hoener, N. Berrah, C. Roedig, and L. F. DiMauro, J. Phys. B: At. Mol. Opt. Phys. **46**, 164003 (2013).
[16]J. Feldhaus, M. Krikunova, M. Meyer, T. Möller, R. Moshammer, A. Rudenko, T. Tschentscher, and J. Ullrich, J. Phys. B: At. Mol. Opt. Phys. **46**, 164002 (2013).
[17]V. Lyamayev, Y. Ovcharenko, R. Katzy, M. Devetta, L. Bruder, A. LaForge, M. Mudrich, U. Person, F. Stienkemeier, M. Krikunova, T. Möller, P. Piseri, L. Avaldi, M. Coreno, P. O'Keeffe, P. Bolognesi, M. Alagia, A. Kivimäki, M. D. Fraia, N. B. Brauer, M. Drabbels, T. Mazza, S. Stranges, P. Finetti, C. Grazioli, O. Plekan, R. Richter, K. C. Prince, and C. Callegari, J. Phys. B: At. Mol. Opt. Phys. **46**, 164007 (2013).
[18]M. Yabashi, H. Tanaka, T. Tanaka, H. Tomizawa, T. Togashi, M. Nagasono, T. Ishikawa, J. R. Harries, Y. Hikosaka, A. Hishikawa, K. Nagaya, N. Saito, E. Shigemasa, K. Yamanouchi, and K. Ueda, J. Phys. B: At. Mol. Opt. Phys. **46**, 164001 (2013).
[19]T. E. Glover, D. M. Fritz, M. Cammarata, T. K. Allison, S. Coh, J. M. Feldkamp, H. Lemke, D. Zhu, Y. Feng, R. N. Coffee, M. Fuchs, S. Ghimire, J. Chen, S. Shwartz, D. A. Reis, S. E. Harris, and J. B. Hastings, Nature **488**, 603 (2012).
[20]T. E. Glover, M. P. Hertlein, S. H. Southworth, T. K. Allison, J. van Tilborg, E. P. Kanter, B. Krässig, H. R. Varma, B. Rude, R. Santra, A. Belkacem, and L. Young, Nat. Phys. **6**, 69 (2010).
[21]J. Andreasson, B. Iwan, A. Andrejczuk, E. Abreu, M. Bergh, C. Caleman, A. J. Nelson, S. Bajt, J. Chalupsky, H. N. Chapman, R. R. Fäustlin, V.

Hájková, P. A. Heimann, B. Hjörvarsson, L. Juha, D. Klinger, J. Krzywinski, B. Nagler, G. K. Pálsson, W. Singer, M. M. Seibert, R. Sobierajski, S. Toleikis, T. Tschentscher, S. M. Vinko, R. W. Lee, J. Hajdu, and N. Timneanu, Phys. Rev. E **83**, 016403 (2011).
[22]M. Bergh and N. Tîmneanu, Phys. Rev. E **77**, 026404 (2008).
[23]M. Beye, O. Krupin, G. Hays, A. H. Reid, D. Rupp, S. de Jong, S. Lee, W. S. Lee, Y. D. Chuang, R. Coffee, J. P. Cryan, J. M. Glownia, A. Foehlisch, M. R. Holmes, A. R. Fry, W. E. White, C. Bostedt, A. O. Scherz, H. A. Durr, and W. F. Schlotter, Appl. Phys. Lett. **100**, 121108 (2012).
[24]R. Riedel, A. Al-Shemmary, M. Gensch, T. Golz, M. Harmand, N. Medvedev, M. J. Prandolini, K. Sokolowski-Tinten, S. Toleikis, U. Wegner, B. Ziaja, N. Stojanovic, and F. Tavella, Nat. Commun. **4**, 1731 (2013).
[25]M. Harmand, R. Coffee, M. R. Bionta, M. Chollet, D. French, D. Zhu, D. M. Fritz, H. T. Lemke, N. Medvedev, B. Ziaja, S. Toleikis, and M. Cammarata, Nature Photon. **7**, 215 (2013).
[26]M. R. Bionta, N. Hartmann, M. Weaver, D. French, D. J. Nicholson, J. P. Cryan, J. M. Glownia, K. Baker, C. Bostedt, M. Chollet, Y. Ding, D. M. Fritz, A. R. Fry, D. J. Kane, J. Krzywinski, H. T. Lemke, M. Messerschmidt, S. Schorb, D. Zhu, W. E. White, and R. N. Coffee, Rev. Sci. Instrum. **85**, 083116 (2014).
[27]N. Hartmann, W. Helml, A. Galler, M. R. Bionta, J. Grünert, S. L. Molodtsov, K. R. Ferguson, S. Schorb, M. L. Swiggers, S. Carron, C. Bostedt, J. C. Castagna, J. Bozek, J. M. Glownia, D. J. Kane, A. R. Fry, W. E. White, C. P. Hauri, T. Feurer, and R. N. Coffee, Nature Photon. **8**, 706 (2014).
[28]S. Eckert, M. Beye, A. Pietzsch, W. Quevedo, M. Hantschmann, M. Ochmann, M. Ross, M. P. Minitti, J. J. Turner, S. P. Moeller, W. F. Schlotter, G. L. Dakovski, M. Khalil, N. Huse, and A. Föhlisch, Appl. Phys. Lett. **106**, 061104 (2015).
[29]R. Torre, *Time-resolved Spectroscopy in Complex Liquids: An Experimental Perspective*, 1st ed., edited by R. Torre (Springer-Verlag, 2007).
[30]B. Pasenow, J. V. Moloney, S. W. Koch, S. H. Chen, A. Becker, and A. Jaroń-Becker, Opt. Express **20**, 2310 (2012).
[31]S. Pabst, Eur. Phys. J. Spec. Top. **221**, 1 (2013).
[32]M. Mittendorff, T. Winzer, E. Malic, A. Knorr, C. Berger, W. A. de Heer, H. Schneider, M. Helm, and S. Winnerl, Nano Lett. **14**, 1504 (2014).
[33]G. E. Jellison and L. A. Boatner, Phys. Rev. B **58**, 3586 (1998).
[34]I. H. Lee, K. J. Yee, K. G. Lee, E. Oh, D. S. Kim, and Y. S. Lim, J. Appl. Phys. **93**, 4939 (2003).
[35]C. Aku-Leh, J. Zhao, R. Merlin, J. Menéndez, and M. Cardona, Phys. Rev. B **71**, 205211 (2005).
[36]F. D. J. Brunner, J. A. Johnson, S. Grübel, A. Ferrer, S. L. Johnson, and T. Feurer, J. Opt. Soc. Am. B **31**, 904 (2014).
[37]J. A. Johnson, F. D. J. Brunner, S. Grübel, A. Ferrer, S. L. Johnson, and T. Feurer, J. Opt. Soc. Am. B **31**, 1035 (2014).
[38]See supplementary material at http://dx.doi.org/10.1063/1.4917506 for fits and fitting parameters, Jones matrix treatment of the photodiode signals, and heterodyne measurements.
[39]A. Leonov, D. Ksenzov, A. Benediktovitch, I. Feranchuk, and U. Pietsch, Int. Union Crystallogr. **1**, 402 (2014).
[40]A. Grüneis, R. Saito, G. G. Samsonidze, T. Kimura, M. A. Pimenta, A. Jorio, A. G. Souza, G. Dresselhaus, and M. S. Dresselhaus, Phys. Rev. B **67**, 165402 (2003).
[41]E. Malic, T. Winzer, E. Bobkin, and A. Knorr, Phys. Rev. B **84**, 205406 (2011).
[42]T. Winzer, A. Knorr, M. Mittendorff, S. Winnerl, M.-B. Lien, D. Sun, T. B. Norris, M. Helm, and E. Malic, Appl. Phys. Lett. **101**, 221115 (2012).
[43]S. Mitsubori, I. Katayama, S. H. Lee, T. Yao, and J. Takeda, J. Phys.: Condens. Matter **21**, 064211 (2009).